Published in final edited form as:
J Neurosci Res. 2011 December ; 89(12): 2052–2067. doi:10.1002/jnr.22663.

Reduced gap junctional communication among astrocytes in experimental diabetes: Contributions of altered connexin protein levels vs. oxidative-nitrosative modifications

Kelly K. Ball[1], **Lamia Harik**[1], **Gautam K. Gandhi**[2], **Nancy F. Cruz**[1], and **Gerald A. Dienel**[1,2]

[1] Department of Neurology, University of Arkansas for Medical Sciences, Little Rock, Arkansas, 72205, USA

[2] Department of Physiology and Biophysics, University of Arkansas for Medical Sciences, Little Rock, Arkansas, 72205, USA

Abstract

Experimental diabetes increases production of reactive oxygen-nitrogen species and inhibits astrocytic gap junctional communication in tissue culture and brain slices from streptozotocin (STZ)-diabetic rats by unidentified mechanisms. Relative connexin (Cx) protein levels were assessed by Western blotting using extracts from cultured astrocytes grown in high (25 mmol/L) or low (5.5 mmol/L) glucose for 2–3 weeks and STZ-diabetic rat brain. Chemiluminescent signals for diabetic samples were normalized to those of controls on the same blot and same protein load. Growth in high glucose did not alter relative Cx26 level, whereas Cx30 and glyceraldehyde-3-phosphate dehydrogenase (GAPDH) were reduced by ~30% and Cx43 increased ~1.9-fold. In the inferior colliculus of STZ-diabetic rats, Cx30 and Cx43 levels in three of four rats were half those of controls, whereas GAPDH and actin were unaffected. Diabetes did not affect levels of Cx30, Cx43, and GAPDH in cerebral cortex, but actin level rose 24%. Cx43 was predominantly phosphorylated in control and diabetic samples, so reduced dye transfer is not due to overall dephosphorylation of Cx43. Astrocytic growth in high glucose reduced dye-labeled area by 75%, but 10 min treatment with dithiothreitol restored normal dye transfer. In contrast, nitric oxide donors inhibited dye transfer among astrocytes grown in low glucose by 50–65% within 1h. Thus, modifications arising from oxidative-nitrosative stress, not altered connexin levels, may underlie reduced dye transfer among severely-hyperglycemic cultured astrocytes, whereas both oxidative-nitrosative stress and regionally-selective down-regulation of connexin protein content may affect gap junctional communication in brain of STZ-diabetic rats.

Keywords

astrocyte; connexin; diabetes; gap junction; housekeeping proteins; hyperglycemia; oxidative-nitrosative stress; streptozotocin; Western blot

INTRODUCTION

Experimental diabetes is associated with large increases in glucose levels in blood and body tissues, including brain (Gandhi et al., 2010). Pathophysiological changes associated with diabetes include non-specific glycation reactions of glucose, increased sorbitol production,

Corresponding Author: Gerald A. Dienel, Ph.D. University of Arkansas for Medical Sciences, Department of Neurology, Slot 830, Shorey Building, Room 715, 4301 West Markham Street, Little Rock, AR 72205, Phone (501) 603-1167, Fax (501) 296-1495, gadienel@uams.edu.

oxidative-nitrosative stress, endogenous antioxidant depletion, enhanced lipid peroxidation, metabolic changes, altered hormonal responses, cardiovascular disease, kidney damage, poor wound healing, and cataract formation (Brownlee, 2005). Peripheral complications of diabetes are much more severe and debilitating than those involving the central nervous system (Little et al., 2007), but sensory processing and cognitive systems in the central nervous system can be impaired by diabetes. For example, decrements in cognition, learning, and brain function have been documented in diabetic patients and in animal models of diabetes (McCall, 1992, 2004, 2005; Mooradian, 1997; Biessels et al., 1998; Kamal et al., 1999; Allen et al., 2004; Sima et al., 2004; Biessels et al., 2005; Biessels and Gispen, 2005; Kamal et al., 2006; Huber et al., 2006; Brands et al., 2007; DCCT/EDIC, 2007; Manschot et al., 2008; Roberts et al., 2008; Kodl and Seaquist, 2008). Diabetic patients have longer latencies for visual and auditory evoked potentials (Buller et al., 1988; Di Mario et al., 1995; Diaz de Leon-Morales et al., 2005) and acquire hearing deficits (Tay et al., 1995; Frisina et al., 2006; Vaughn et al., 2006, 2007). Diabetic rats also have abnormal visual and auditory evoked potentials (Buller et al., 1986; Rubini et al., 1992; Biessels et al., 1999; Manschot et al., 2003), and rodent models may be useful to understand how diabetes affects the CNS and to develop therapeutic approaches.

The inferior colliculus is a midbrain auditory-processing structure that has the highest metabolic and blood flow rates in the brain (Sokoloff et al., 1977; Gross et al., 1987). Astrocytes in the rat inferior colliculus are highly coupled by gap junctions (Ball et al., 2007), and rapid spreading and release of labeled metabolites of glucose within the inferior colliculus during acoustic stimulation is reduced by treatment with gap junction and lactate transport blockers (Cruz et al., 2007; Dienel and Cruz, 2008), supporting our hypothesis that metabolite trafficking among astrocytes is high in this brain structure. We recently showed that gap junctional communication among astrocytes is disrupted by prolonged hyperglycemia and diabetes. The area labeled by gap junction-mediated dye transfer is reduced by about 50% in (i) cerebral cortical astrocytes grown in high-glucose (25 mmol/L) compared to that in low (5.5 mmol/L) glucose cultures and (ii) in astrocytes in slices of the inferior colliculus of streptozotocin (STZ)-diabetic rats compared to age-matched, vehicle-injected controls (Gandhi et al., 2010). These findings are consistent with earlier reports of reduced transfer through gap junctional pores in other cell types (e.g., Inoguchi et al., 1995; Stalmans and Himpens, 1997; Kuroki et al., 1998; Oku et al., 2001; Sato et al., 2002; Li et al., 2003), suggesting that trafficking of ions, signaling molecules, and metabolites among cells linked by gap junctions is vulnerable to prolonged hyperglycemia and that this deficit could affect many tissues in diabetic patients.

The goal of the present study was to determine if reduced levels of connexin (Cx) proteins are a major cause of impairment of transcellular trafficking among astrocytes in cultured astrocytes and STZ-diabetic rats, or whether other factors may also be involved. We report that connexin levels were altered in astrocytes cultured in high glucose, but these changes do not explain reduced dye transfer. Normal dye transfer among astrocytes grown in high-glucose, could, however, be restored by brief treatment with dithiothreitol. On the other hand, dye transfer among astrocytes grown in low glucose was reduced by nitric oxide donors, consistent with a role for oxidative-nitrosative stress. In the inferior colliculus of streptozotocin (STZ)-diabetic rats, levels of Cx30 and Cx43 were reduced and may contribute to reduced dye transfer, along with oxidative-nitrosative stress. In contrast, connexin levels were normal in cerebral cortex, raising the possibility of regional differences in the effects of diabetes on astrocytes.

MATERIALS AND METHODS

Materials

Dulbecco's modified Eagle's medium (DMEM; low glucose, catalog number 12320-032 and high glucose, #12430-054), penicillin-streptomycin, Amphotericin B, trypsin, phosphate-buffered saline, pH 7.4 (PBS; Gibco/Invitrogen #10010), affinity-purified rabbit polyclonal antibodies against Cx43 (#71-0700), Cx30 (#71-2200), Cx26 (#51-2800), and goat anti-rabbit IgG-horseradish peroxidase (HRP)-conjugated secondary antibody (Zymed-Invitrogen #81-6120 or Invitrogen #G21234) were obtained from Invitrogen (Carlsbad, CA). Fetal bovine serum (FBS) was from Hyclone (Logan, UT). Dibutyryl cyclic-adenosine monophosphate (dBcAMP), L-leucine methyl ester hydrochloride (L-LME), diethanolamine (D-8885), alkaline phosphatase type VII-T (P6774), bovine serum albumin, antibodies against glyceraldehyde-3-phosphate dehydrogenase (GAPDH, G9545) and actin (A2066), poly-D-lysine (P0899), Lucifer yellow VS (LYVS, dilithium salt), dithiothreitol, sodium nitroprusside, and spermine-NO were from Sigma-Aldrich (St. Louis, MO). Protein assay reagent, Precision Plus Protein all blue standards, and precast gels (4–15% linear gradient gels, 10% Ready Tris-HCl gels, and 10% MiniProtean TGX gels) were from BioRad (Hercules, CA). Six-well culture plates were purchased from Fisher Scientific (Pittsburgh, PA) and were coated with poly-D-lysine prior to use (Freshney, 2000). Complete protease inhibitor cocktail was from Roche Diagnostics GmbH (Mannheim, Germany), T-PER tissue protein extraction reagent from Pierce (Rockford, IL), polyvinylidene fluoride (PVDF) membranes from Millipore (Billerica, MA), and ChemiGlow Western blotting detection reagent from Alpha Innotech Corp. (San Leandro, CA).

Astrocyte culture

Cultured astrocytes were prepared by previously-established procedures (Hertz et al., 1998), with small modifications. In brief, Hanover-Wistar rat pups <2 days of age (Taconic Farms, Germantown, NY) were decapitated, and cerebral cortical tissue above and lateral to the lateral ventricles was aseptically dissected and placed in Dulbecco's modified Eagle's medium (DMEM) containing 5.5 mmol/L glucose plus 10% fetal bovine serum (FBS), 100 units/ml of penicillin and 100μg/ml of streptomycin (P/S) plus 0.1 mmol/L L-leucine methyl ester (L-LME). L-LME was used to minimize the presence of microglial cells (Simmons and Murphy, 1992; Hamby et al., 2006; Esen et al., 2004, 2007). The meninges and associated blood vessels were carefully removed using jeweler's forceps and by rolling the tissue several times on sterile nitex mesh. The tissue was placed in fresh DMEM (5.5 mmol/L glucose) with 10% FBS, P/S, and L-LME and disassociated by repeated pipetting with a 10 mL pipette until homogenized. Then the cells were seeded into T-75 tissue culture flasks and maintained at 37°C in a 5% CO_2/95% O_2 air atmosphere, humidified incubator. After 24 hours, cells were washed with PBS to dislodge microglia and oligodendrocytes, and fresh DMEM (5.5 mmol/L glucose) with 10% FBS, P/S, and L-LME was added. The culture medium was changed every 3–4 days thereafter, and after two weeks, the confluent cells were trypsinized and re-plated in poly-D-lysine-coated 6-well plates. The medium, with 2.5μg/ml amphotericin B added, was changed the next day to clear away any cell debris. Once the cells were confluent, all wells were treated with culture medium supplemented with 2.5μg/ml amphotericin B (Esen et al., 2004) and 0.25 mmol/L dBcAMP (Hertz et al., 1998). dBcAMP is used to induce morphological and some biochemical differentiation of the astrocytes (e.g., increased content of glial fibrillary acidic protein (GFAP) and development of some enzymes), increase longevity of the cultures, and reduce any macrophage contamination (Schousboe et al., 1980; Hertz et al. 1998). After 24-hour exposure to dBcAMP, cells were cultured in either 5.5 mmol/L (low) glucose or 25 mmol/L (high) glucose media plus 0.25 mmol/L dBcAMP and amphotericin B for two to three weeks. In our previous study that used identical procedures (Gandhi et al., 2010), purity of

the cultures was based on expression of GFAP (an astrocyte marker) that was detected in >90% of the cells.

Streptozotocin (STZ)-induced diabetes

Brain tissue samples were from the same STZ-diabetic and age-matched, vehicle-injected control rats used in our previous study (Gandhi et al., 2010) for assays of dye transfer and reactive oxygen-nitrogen species in slices of inferior colliculus. In brief, these rats were given a single intraperitoneal injection of STZ (65 mg/kg in 33 mmol/l citrate-buffered saline, pH 4.5) or vehicle. Three days later, the hyperglycemic rats were identified by assay of tail blood glucose levels. During the subsequent 13–20 week interval, the body weight of diabetic rats averaged 53% of age-matched controls. At time of euthanasia (20–24 weeks), arterial plasma glucose levels (mean ± SD, mmol/L) were 33.1 ± 5.2 and 8.0 ± 0.9 for diabetic and control rats, respectively, whereas arterial plasma lactate levels were similar (2.2 ± 0.7 and 2.2 ± 0.4, respectively). Glucose concentrations in cerebral cortex in two of our diabetic rats were 8.2 and 6.8 μmol/g compared to 2–3 μmol/g in normal rat brain (see Table 1 in Gandhi et al., 2010). After euthanasia, one inferior colliculus and each hemisphere of cerebral cortex were dissected out and immediately frozen on dry ice and stored at −80°C.

Extraction procedures

Cultured astrocytes—Each 6-well plate was placed on ice, the culture medium was removed from one well at a time, cells were washed with sterile, chilled PBS (2 ml/well), the PBS was aspirated and 500μl of freshly-prepared, ice-cold extraction buffer (pH 7.4) was added to the well, and cells were dislodged using a sterile, disposable cell scraper. The extraction buffer contained 0.1% sodium dodecyl sulfate (SDS), 1% Triton-X, 10 mmol/L Na fluoride, 1 mmol/L Na orthovanadate, 0.1 mmol/L neocuproine, 1 mmol/L EDTA, complete protease inhibitor cocktail (1:25 dilution) in 20 mmol/L PBS or 25 mmol/L HEPES with 50 mmol/L NaCl. Then the next well was washed, the PBS aspirated, and the cell lysate from the previous well was transferred to it, followed by scraping of the cells. Serial extractions of cells from 3 wells were combined in the 500μl extraction buffer; this volume was used to ensure protein denaturation and prevent proteolysis when cells are scraped. Serial extractions increased the protein concentration in the pooled sample to appropriate levels for gel analysis. Lysates were placed on ice, vortexed every 5 min for 30 min, centrifuged at 16,000 g at 4°C for 20 min, and supernatant fractions stored at −80°C.

Brain tissue—Samples were extracted with ice-cold, freshly-prepared extraction buffer (20 ml/g tissue) comprised of T-PER tissue protein extraction reagent to which were added Na fluoride (10 mmol/L), Na orthovanadate (1 mmol/L), neocuproine (0.1 mmol/L), and complete protease inhibitor cocktail (1:25 dilution). Brain tissue was homogenized on ice using a motor-driven Teflon pestle (inferior colliculus) or Polytron laboratory homogenizer (Kinematica AG, Switzerland) (cerebral cortex), then centrifuged at 16,000 g for 5 min at 4°C, and supernatant fractions stored at −80°C.

Protein assays

The protein concentration of each extract sample was determined in triplicate in 96-well microplates using the Bio-Rad protein assay reagent and measuring absorbance at 595nm. The protein concentration was calculated from the standard curve assayed in parallel and constructed with known amounts of bovine serum albumin that were appropriately diluted in the extraction buffer corresponding to that sample set.

SDS-PAGE and Western blotting

The samples were thawed, vortexed at room temperature, mixed with an equal volume freshly-prepared sample buffer (Laemmli buffer plus 5% 2-mercaptoethanol), and repeatedly vortexed at room temperature. The measured protein concentration in each sample was used to calculate the volume loaded onto each gel lane so that defined protein amounts, generally within the range 2.5–20 μg, were loaded per lane.

Samples from seven independent batches of astrocytes, each derived from a different litter, were assayed. Each gel contained molecular weight standards and a pair of samples from the same culture batch and grown in parallel in either high or low glucose. Replicate lanes for each sample were loaded with the same amount of protein or 2–3 different protein levels. Pairs of samples from diabetic and control rats were similarly assayed, and, since the number of brain tissue samples was smaller than that of cultured cells, replicate assays for proteins of interest were also carried out with all diabetic and control samples on the same gel. Calibrated pipettes (Precision Laboratory Support, Hacienda Heights, CA) were used for all procedures, and their accuracy and reproducibility (coefficients of variation are typically <1–2%) are periodically verified by laboratory personnel; particular care was taken when pipetting the glycerol- and detergent-containing samples. The 4–15% gradient resolving gels were used for samples from cultured astrocytes; 10% TGX gels were used for brain tissue. Proteins were separated using a Mini Protean II Cell (BioRad) at 80V.

Proteins were transferred from the resolving gel to a methanol-activated PVDF membrane at 76V for 50 min using a Mini Trans-blot Electrophoretic Transfer Cell (Bio-Rad), and membranes were blocked in 5% blotto (5% milk in TBST [0.05% Tween-20 in TBS, 20 mmol/L Tris 0.5 mol/L NaCl, pH 7.5]) for 1 h at room temperature with constant, gentle shaking. Then the membranes were incubated overnight at 4°C with primary antibodies diluted in 1% blotto. After washing 3 times (10 min/wash) with TBST, membranes were incubated in secondary antibody diluted in 1% blotto for 1 h at room temperature with gentle shaking. Antibody dilutions were: anti-Cx26 (1:500), anti-Cx43 (1:10,000), anti-Cx30 (1:500), anti-GAPDH (1:40,000), anti-actin (1:500), goat anti-rabbit IgG-HRP (1:20,000). The membranes were washed 3 times (15–30 min/wash) with TBST, and the bands were detected with ChemiGlow Western blotting detection reagent (2 ml/membrane) and imaged with a BioRad ChemiDoc XRS system. The tiff images of samples from cultured astrocyte were analyzed with MCID Elite™ software (7.0 Rev. 1.0 build 207; InterFocus Imaging Ltd, Cambridge, England), whereas those for alkaline phosphatase assays and brain tissue samples were analyzed with BioRad Image Lab Software (version 2.0.1). The units for chemiluminescence signals differed for the two software programs but preliminary assays showed that analysis of the same sample with both software programs gave equivalent results. Chemiluminescent signals were background-subtracted, and, for each protein amount loaded on a gel, the signal for each high glucose or diabetic sample was normalized by dividing by the value for the same protein in the corresponding low glucose or control tissue sample on the same blot. The mean diabetes/control ratio of all replicate assays of each sample pair was used to calculate the overall normalized mean value for all cultures or brain samples for each protein of interest. After assays of signal intensities in blots from cultured astrocytes, the membranes were incubated in freshly-prepared stripping buffer (100 mmol/L mercaptoethanol, 2% SDS, 62.5 mmol/L Tris-HCl, pH 6.7) at 50°C for 30 min with gentle agitation and then re-probed with antibodies against GAPDH. For some rat brain samples, stripping was also used to assay GAPDH and actin; in other assays, these proteins were assayed on blots of separate gels.

Alkaline phosphatase treatment

Cell lysates from astrocyte cultures (100 μg protein) grown in high and low glucose and inferior colliculus and cerebral cortex from diabetic and control rats (50 μg protein) were incubated in buffer (100 mmol/L diethanolamine and 2 mmol/L $MgCl_2$, pH 10) without or with 100 units of alkaline phosphatase in a water bath at 37°C for 1h; the samples remained at room temperature overnight, and were incubated at 37°C for another hour the next morning. Each sample was then added to Laemmli sample buffer, mixed, and assayed by SDS-PAGE on 10% Ready Gels or 10% TGX gels and Western blotting for Cx43.

Dye transfer assays

Cultured astrocytes grown on coverslips were visualized under differential interference contrast using a Nikon Eclipse E600 microscope (Melville, NY) equipped with a Nikon Fluor 40× (numerical aperture 0.80) objective and Photometrics CoolSNAP ES camera (Roper Scientific, Atlanta, GA). Micropipettes with 12–14 MΩ resistance (tip inner/outer diameters, 1.0/1.8 μm) were constructed from borosilicate glass using a P97 pipette puller (Sutter Instruments, Novato, CA) and filled with a test solution containing 4% (62 mmol/L) Lucifer yellow VS dissolved in the following solution (composition in mmol/L): 21.4 KCl, 0.5 $CaCl_2$, 2 $MgCl_2$, 5 EGTA, 2 ATP, 0.5 GTP, 2 ascorbate, 10 HEPES, pH 7.2. Lucifer yellow VS labels nuclei plus cytoplasm, simplifying identification of labeled cells and counts of cell number compared to Lucifer yellow CH that mainly labels the cytoplasm; both tracers are used to evaluate dye transfer (Ball et al., 2007 and references cited therein). The osmolarity of each solution was measured (Osmette II, Precision Systems, Natick MA) and adjusted to 305–320 mOsm/L with sucrose. Single astrocytes were impaled with micropipettes using a MP-225 manipulator (Sutter Instruments, San Francisco, CA), the dye diffused into the cell for 2 min, and the pipette removed. Fluorescence intensity, background subtraction, and dye-labeled area was determined with MetaVue software (Ball et al., 2007; Gandhi et al., 2010).

Statistics

All statistical analyses were performed with GraphPad Prism® software, version 5.02 (GraphPad Software. La Jolla, CA); $p \leq 0.05$ was considered to be statistically significant. Significant outliers from the rest of the samples in a group were identified with the Grubbs' test (http://GraphPad.com/quickcalcs/grubbs2.cfm).

RESULTS

Technical aspects of the SDS-PAGE/Western blotting assays

Sample preparation—Previous reports of assays for Cx26 (Brissette et al., 1991; Nagy et al., 2001), Cx30 (Rash et al., 2001), and Cx43 (Invitrogen product manual for rabbit anti-Cx43, catalog number 71-0700; http://tools.invitrogen.com/content/sfs/manuals/710700_Rev1008.pdf) stated that samples were not boiled before gel loading. When Western blots from boiled and non-boiled aliquots of the same samples were assayed in parallel on the same gel, boiling prior to loading on the gel was found to reduce the levels of Cx43, Cx26, GAPDH, and actin, with small, if any, effects on Cx30 (Table 1a). Subsequent samples were not boiled.

Protein loading and normalization of chemiluminescent signals—Loading controls are commonly used to minimize variability of signals on different blots by dividing the signal for a protein of interest by that of a housekeeping protein in the same sample. These ratios can be used for comparisons if (i) the concentration of the internal reference protein is not altered by experimental conditions, and (ii) the reference signal is sufficiently

sensitive to correct for variations in protein amount. To avoid the issue of reference protein stability, the present study normalized signals from proteins of interest in experimental samples to those of the same protein in control samples that were assayed in the same blot and at the same protein load. When the diabetic/control ratio is calculated, protein amount cancels out (as would the signal for a loading control if its value were identical for both samples), i.e., [(signal for protein in a high glucose sample/μg protein loaded)]/[(signal for protein in a low glucose sample/μg protein loaded)].

The above normalization procedure requires that signals from the same protein load are equivalent, so the overall reproducibility of Western blot assays was first evaluated by pipetting duplicate samples of the same protein amount into different lanes of the same gel, then various sample pairs were assayed on different gels. Duplicate assays of 12 samples for Cx43 yielded a coefficient of variation of 8%, and duplicate assays for GAPDH were also in close agreement, whereas those for actin were more variable (Table 1b). Thus, protein loading is sufficiently reproducible to enable use of ratios of signals from different samples on the same gel and same protein amount for gel-to-gel comparisons. Reproducibility of diabetic/control ratios obtained from 2–5 different gels/blots are shown in Table 1c. The coefficients of variation or percent difference (for two ratio values) were lowest for pairs of samples assayed for Cx43 and Cx30; most replicates agreed within the range of about 2–11%. In contrast, the coefficients of variation obtained for GAPDH and actin were higher, ranging from 12%–43% (Table 1c). These findings validate our normalization procedure for assays of relative changes in connexin protein levels.

Specificity and linearity of immunoassays—Representative Western blots of non-boiled samples (Fig. 1) show that, after optimization of antibody dilutions, immunoreactive Cx26, Cx30, and Cx43 protein are readily detectable in extracts of cultured astrocyte. One major immunoreactive protein band was detected in blots for Cx30, Cx43, and GAPDH, whereas Cx26 had two bands; the larger one probably represents a dimer that has been observed with the same antibody against Cx26 in blots of liver and leptomeningial tissue (Nagy et al. 2001).

Good correlations between chemiluminescent signal magnitude and loaded protein amount were observed for most samples over the range of 2.5–20 μg (Fig. 2). Plots of the paired high and low glucose samples usually, but not always, yielded approximately parallel lines. Occasionally, some samples had divergent values (e.g., Fig. 2A, 10 μg loads for Cx26) or the slopes of the plots that were not parallel (e.g., Fig. 2D, GAPDH). However, most or all of the values for a given group were either higher or lower than respective value for the other group. The slopes of the plots of chemiluminescent signal vs. amount of extract protein loaded on the gel varied for different proteins of interest; those with a steeper slope are most sensitive to protein amount (Fig. 2). Most profiles showed that increases in the protein amount yielded a smaller fractional increase in the chemiluminescent signal (i.e., doubling the protein did not necessarily double the signal), as has been reported by other investigators for various proteins (see Discussion).

Growth of cultured astrocytes in high glucose affects levels of specific proteins

Connexin levels were assayed in 7 batches of cultured astrocytes exposed to 2–3 weeks of low or high glucose, corresponding to the time interval during which dye transfer is reduced by about 50% (Gandhi et al., 2010). Differences among batches of cultured astrocytes were minimized by parallel assays of the paired high-low glucose cultures from each culture batch on the same blot.

Two immunoreactive bands for Cx26 were detected (Fig. 1), and, because variability could arise if some Cx26 protein shifted between the two bands in different samples, signals from

both bands were combined and the high/low glucose ratio calculated from composite values; the mean ratio was close to 1.0 (Fig. 3). The high/low glucose ratios were also analyzed for each of the Cx26 bands, the ratios were similar and not different from 1.0 (data not shown). The levels of Cx30 and GAPDH were reduced by about 30% in the high compared to low glucose cultures (Fig. 3). Batch-to-batch variability was greatest for Cx43 and one high value increased the overall mean ratio, which averaged about 1.9 (Fig. 3). If Cx signal intensities were normalized to that of GAPDH, the relative signal intensities of Cx 26 and Cx43 in the high glucose cultures would have been inflated and the reduced expression of Cx 30 would have been masked.

The effect of culture duration was assessed by plotting the high/low glucose ratio as function of culture time for each protein of interest (not shown). The high/low glucose ratio for Cx26 tended to be slightly below 1.0 at 15 days and to increase with time at 21 days ($r^2 = 0.833$), whereas those for Cx30, Cx43, and GAPDH did not show time dependence.

STZ-diabetes down-regulates Cx30 and Cx43 levels in the inferior colliculus but not cerebral cortex

Diabetic-control pairs of brain tissue samples from different rats were initially assayed on different blots, as for the tissue culture samples. However, one pair from the inferior colliculus had a high ratio for Cx 43 and Cx30 (Pair 1, Table 1c) compared to the other three pairs (i.e., Pairs 2–4, Table 1c), and this approach is limited by lack of comparison of all samples in the same experimental group. Because the number of brain tissue samples (n=3–4 diabetic and 3–4 controls) was smaller than those for tissue culture (n=7 high glucose and 7 low glucose batches), the brain samples were re-analyzed by loading all samples for each protein of interest on the same gel (Fig. 4). When diabetic/control ratios for the same samples were calculated, the results were the same for both approaches (Table 1c, Fig. 4). The levels of Cx30 and Cx43 protein in the inferior colliculus of STZ-diabetic brain were about half those of controls in three of the four samples, whereas one rat had Cx30 and Cx43 levels double those of the respective control values (Fig. 4A–a, b). In contrast, the levels of GAPDH and actin were similar in all samples from each diabetic and control rat (Fig. 4A–c) indicating that the upregulation of Cx43 and Cx30 in that animal was not related changes in levels of two housekeeping proteins. Thus, Cx30 and Cx43 levels were reduced in 3 of 4 diabetic inferior colliculi, regardless of whether the diabetic/control ratios were expressed relative to protein load (Fig. 4A) or normalized to either of the two internal controls that were assayed on different gels (not shown; see Fig. 4 legend).

In cerebral cortex, levels of Cx30 and Cx43 were compared on the same gels/blots and were similar in diabetic compared to control samples (Fig. 4B–a, b). Cx26 was not detected in extracts of inferior colliculus or cerebral cortex from STZ-diabetic or control rats (data not shown). GAPDH levels were also similar in diabetic and control cerebral cortex, whereas actin was about 24% higher in the diabetic compared to control tissue (Fig. 4B–c). The relative levels of the two connexin proteins was not different from control when normalized to protein amount, GAPDH, or actin. Note that the signal intensity for actin was similar to that of GAPDH in cerebral cortex (Fig. 4B–c), whereas it was much lower than GAPDH in the inferior colliculus (Fig. 4A–c).

Cx43 is not extensively dephosphorylated in experimental diabetes

Cx43 in brain tissue is phosphorylated (e.g., Hossain et al., 1994; Ball et al., 2007; and references cited in these studies), and dephosphorylation of Cx43 is associated with uncoupling of gap junctional communication (e.g., Li and Nagy, 2000; Li et al., 2005; and references cited therein). Because discrete bands for phosphorylated Cx43 isoforms were not resolved in assays using either a home-made 10% gel (data not shown) or 4–15% gradient

gels, 10% Ready gels, or 10% TGX gels (Figs. 1–4), the overall phosphorylation state of Cx43 was assessed by incubating samples with or without alkaline phosphatase followed by SDS-PAGE on 10% Ready or TGX gels and Western blotting. Enzymatic treatment shifted the Cx43 bands to a lower apparent molecular weight in samples from low and high glucose cultures and from control and diabetic rats (Fig. 5). Cx43 was not largely dephosphorylated in the high-glucose cultures or diabetic rat brain.

Dye transfer among cultured astrocytes is enhanced by a reducing agent and inhibited by nitric oxide donors

Growth of astrocytes for two weeks in high glucose reduced the area labeled by Lucifer yellow by about 75% compared to that for low glucose cultures (Fig. 6, A, B; Table 2). The dye-transfer deficit caused by growth in high glucose was eliminated by treatment with dithiothreitol for 10 min (Fig. 6, B, D; Table 2). Dye-labeled area in astrocytes grown in low glucose for two weeks was reduced by one hour exposure to nitric oxide donors, nitroprusside and spermine-NO (by 65 or 45%, respectively; Fig. 6, A, C; Table 2). Variability of the extent of dye transfer (Table 2) was taken into account by carrying out many assays per experimental group and having parallel sets of control and test cells for each condition.

DISCUSSION

Technical aspects of Western blotting assays

Protein loading—Many variables can affect Western blotting results, ranging from sample preparation, protein loading, electrophoretic separation and transfer of proteins from gels to blotting membranes, immunoassays, signal detection procedures, protein loss during stripping of blots, and signal normalization to an internal reference (Alegria-Schaffer et al., 2009). Variability due to protein loading (i.e., pipetting samples onto a gel) is relatively small, as documented in the present study (Table 1b) and by Calvo et al. (2008) (signals from six replicates of the same sample applied to one gel had coefficients of variation (cv) ranging from 0.5–2.2%) and Liu and Xu (2006) (cv = 6–10%). Low protein loading variability indicates that other factors are responsible for larger blot-to-blot variations, and that the normalization procedure used in the present study is a valid, perhaps preferable, alternative to use of an internal reference protein.

Stability of reference protein level—GAPDH, actin, and tubulin are often chosen as loading controls, but their use is not appropriate when their levels vary (Calvo et al., 2008; Bauer et al., 2009), such as in the present study and the following examples. (i) β-Tubulin was relatively stable with time after spinal cord injury, whereas β-actin increased after several days (Liu and Xu, 2006). (ii) Tissue-specific differences in the levels of β-actin, GAPDH, and β-tubulin occur in a mouse model for amyotrophic lateral sclerosis (Calvo et al., 2008). (iii) Levels of α-tubulin and GAPDH can change with density of cultured cells (Greer et al., 2010). Also, the relatively high levels of actin and GAPDH and their strong chemiluminescent responses may render them relatively insensitive to differences in loaded protein amount (Dittmer and Dittmer, 2006; Aldridge et al., 2008; Romero-Calvo et al., 2010). Normalization to total protein transferred to blot membranes has the advantage that ratios do not rely on a single protein and any losses due to blot stripping are eliminated. Normalization to total protein is more sensitive to differences in loaded protein amount than actin or GAPDH, but variation associated with protein stains is high, and the protein stain signal is relatively insensitive to protein amount, i.e., the slope of a plot of stain signal vs. loaded protein amount rose only about 1.8–2.5-fold over a 14-fold increase in protein load (Aldridge et al., 2008; Romero-Calvo, 2010). Near-infrared fluorescence imaging can overcome some limitations of chemiluminescent assays by eliminating the time-dependent

chemiluminescence reaction, improving the signal-to-noise ratio, and extending the linear ranges of the signals and the sensitivities to amounts of various proteins (Weldon et al., 2008).

'Housekeeping proteins' are affected by diabetes—GAPDH is a multi-functional protein that catalyzes a key reaction in the glycolytic pathway of glucose metabolism and has also important roles in intracellular signaling, cell death cascades, and neuroprotection (Sen et al., 2009; Tristan et al., 2010). GAPDH is a target of non-enzymatic S-nitrosylation of cysteine by nitric oxide and, after covalent modification, it can have several fates, including transfer into the nucleus and function as an apoptotic signal and mediator of nitrosylation of nuclear proteins (Hara et al., 2006; Hara and Snyder, 2006; Kornberg et al., 2010). After one year of STZ-induced diabetes, rat retina has reduced GAPDH level (normalized to actin), the extent of GAPDH ribosylation and nitration is increased, and nuclear translocation increased (Kanwar and Kowluru, 2009). Nuclear translocation and accumulation of GAPDH also occurs in cultured retinal Müller cells grown in 25 mmol/L glucose (Kusner et al., 2004; Yego et al., 2009; Yego and Mohr, 2010). In experimental diabetes, cellular proteins, including actin, become glycated in pericytes (Chibber et al., 1999) and lung endothelial cells (Ghitescu et al., 2001). GAPDH and actin levels are differentially affected in cultured astrocytes grown in high glucose and in STZ-diabetic rat brain (Figs. 3, 4). Together, the above data indicate that 'loading' standards must be carefully chosen.

Influence of tissue culture conditions and developmental status—The source of cells (species, brain region), culture medium composition, and duration of culture can have a high impact on experimental outcome, and culture conditions may have contributed to some differences between results of our studies and the literature. Little or no Cx30 was detected in cultured astrocytes by Li and Nagy (2000) and Nagy and Rash (2000), whereas Cx30 was readily detectable in our study (Fig. 3) and that by Esen et al. (2007); the basis for these differences is not known. Cx26 is detectable in cultured astrocytes (Fig. 3), but not in inferior colliculus or cerebral cortex of adult brain (Fig. 4). Cx26 is known to be enriched in meninges (e.g., Spray et al., 1991; Nagy et al., 2001; Ball et al., 2007), and meninges was, therefore, carefully removed from brain samples before use for culture studies or adult brain tissue assays. The difference between Cx26 levels in cultured astrocytes and adult brain may be related to development since Cx26 mRNA and protein levels are higher in immature compared to adult brain (Prime et al., 2000; Nagy et al., 2001).

In the present study, cultured astrocytes were treated with cAMP to induce differentiation (Hertz et al., 1998). cAMP is known to influence the cellular distribution and phosphorylation of connexins and the permeability of gap junctions (e.g., Saez et al., 1986; Burt and Spray, 1988; Atkinson et al., 1995; Burghardt et al., 1995; Paulson et al., 2000; TenBroek et al., 2001; Lampe and Lau, 2004). Effects of cAMP added to the medium are not ruled out, but all astrocyte cultures were treated in exactly the same manner except for the medium glucose concentration.

Gap junctional communication in experimental diabetes

Deleterious consequences of growth of neural cells in high glucose—In cultured astrocytes, very high glucose reduces oxidative metabolism of glucose and lactate by 50% (Abe et al., 2006), it markedly increases oxidative stress and impairs gap junctional communication (Gandhi et al., 2010), alters the levels of Cx30, Cx43, and GAPDH (Fig. 3), and amplifies intracellular calcium waves in association with increased expression of P2 receptors and pannexin1 and of $P2X_7$ receptor-pannexin1-mediated ATP release (Thi et al., 2010). Cultured neurons have reduced viability and lower responsiveness to the AMP-

protein activated kinase energy signaling system when grown in high glucose (Kleman et al., 2008). Cultured Schwann cells are negatively affected by hyperglycemia due to altered biosynthesis of arachidonic acid and abnormal protection by antioxidants (Mîinea et al., 2002). Hyperglycemic cell culture conditions are much more severe than the usual diabetic conditions in brain in vivo. Even a low glucose medium, 5–6 mmol/L glucose, is about twice the normal rat brain glucose concentration (i.e., about 2–3 μmol/g) and is equivalent to the glucose level in diabetic in rat brain (see Table 1 in Gandhi et al., 2010); any deleterious effects of low glucose media may, however, not be evident in relatively short-term (<3 week) cultures. In sharp contrast, a culture medium glucose level of 20–25 mmol/L is about 10 times that of normal rat brain and 3 times that of diabetic rat brain (Table 1 of Gandhi et al., 2010). Pathological changes can be observed within days of culture in high glucose in many cell types, raising serious concerns about the normalcy of astrocytes, neurons, oligodendrocytes, microglia, and mixed cultures grown in high glucose (see Discussion in Gandhi et al., 2010).

Cell culture models for diabetes—Short-term culture (days to <1–2 weeks) of cells in low (2–5 mmol/L) compared to high (20–30 mmol/L) glucose is commonly used as a model for diabetes and for testing drugs to reverse or minimize hyperglycemic damage. For example, Hammes et al. (2003) grew bovine aortic endothelial cells in 30 mmol/L glucose for 6 h to 5 days to evaluate pathways related to diabetic vascular damage; benfotiamine was shown to block three major pathways of hyperglycemic damage that become manifest within this short time interval. Many cell types (e.g., astrocytes; pigment epithelial cells and pericytes in the retina; endothelial cells in aorta, retina, and epididymal fat pads; and smooth muscle cells in aorta) exhibit reduced dye transfer after growth in high-glucose media, and, except for astrocytes (Fig. 3), this impairment is associated with reduced levels of Cx43 on Western blots (see below).

Impaired dye transfer among astrocytes—We previously showed that reduced dye-labeled area in astrocytes cultured in high glucose was not due to opening of cell-surface channels and that impairment of dye transfer had a slow onset that lagged behind a rise in production of reactive oxygen-nitrogen species by several days (Gandhi et al., 2010). Once established, inhibition of dye transfer was not reversed by transfer to low glucose medium for two additional weeks even though generation of reactive oxygen-nitrogen species fell to control levels. It could, however, be prevented but not reversed by treatment with a nitric oxide synthase inhibitor or superoxide dismutase mimetic, whereas small molecule chaperones known to help protein folding could both prevent and reverse the decrement in dye transfer (Gandhi et al., 2010).

The results of the present study extend this work by showing that reduced gap junctional communication in high-glucose astrocyte cultures is not due to large decrements in connexin protein levels or to overall dephosphorylation of Cx43 (Figs. 3, 5). Instead, there must be modifications, perhaps related to protein mis-folding, that are quickly reversed by dithiothreitol (Fig. 6, Table 2), yet are quite resistant to actions of intracellular reducing agents, even after generation of reactive oxygen-nitrogen species has subsided for two weeks after transfer to low glucose media. Inhibition of dye transfer in low glucose astrocyte cultures by brief exposure to two nitric oxide donors (Fig. 6, Table 2) and the protective effects of a nitric oxide synthase inhibitor (Gandhi et al., 2010) support the possibility that S-nitrosylation of protein-cysteine residues secondary to oxidative-nitrosative stress underlies high-glucose-induced inhibition of dye transfer. Low dye transfer among astrocytes in slices of inferior colliculus from STZ-diabetic rats is also associated with increased oxidative-nitrosative stress (Gandhi et al., 2010), but in vivo temporal relationships between onset of oxidative stress and inhibition of dye transfer and effects of reducing agents and NO-donors have not yet been assessed in brain slices. Initial results in

STZ-diabetic rat brain revealed reduced connexin levels in the inferior colliculus but not cerebral cortex (Fig. 4), raising the possibility of selective regional vulnerability of intercellular communication among astrocytes in diabetic brain.

Oxidative-nitrosative stress and non-enzymatic glycation, nitration, nitrosylation, and carbonylation reactions are associated with complications of diabetes, and these processes covalently modify proteins. Altered structure may lead to changes in protein level, subcellular localization, or detection by immunoassays and Western blotting if the antigenic site is modified. Exposure of sample extracts to reducing conditions will release NO from cysteine-SNO and preclude detection of protein-S-nitrosylation on Western blots. In retina of diabetic rats and mice and in retinal cells cultured in high glucose, elevated inducible nitric oxide synthase (iNOS) activity is associated with increased production of nitric oxide, which has a role in retinopathy and breakdown of the blood-retinal barrier (Du et al., 2004; Leal et al., 2007). Also, as discussed above, S-nitrosylation of GAPDH increases in vivo in the retina of STZ-diabetic rats and in cultured Müller cells grown in high glucose. Thus, abnormal NO production and S-nitrosylation are components of retinal diabetic pathophysiology in vitro and in vivo; more work is required to evaluate consequences of oxidative-nitrosative stress in diabetic brain.

Cx43 phosphorylation status and impaired dye transfer—Changes in Cx43 phosphorylation can modulate gap junctional permeability, and Cx43 dephosphorylation after hypoxia-ischemia is associated with uncoupling (e.g., Li and Nagy, 2000; Li et al., 2005; Lampe and Lau, 2004; and references cited therein). Cx43 was not markedly dephosphorylated in astrocytes grown in high glucose or in two STZ-diabetic brain regions (Fig. 5), but changes in phosphorylation of specific sites that could alter channel properties remain to be assessed. In cultured aortic smooth muscle cells, a shift to more highly-phosphorylated Cx43 is associated with reduced dye transfer in short-term (2–7-day) high-glucose cultures (Kuroki et al., 1998), whereas in retinal pigment epithelial cells Cx43 was down-regulated by high glucose without a significant change in the phosphorylation state (Malfait et al., 2001). The levels of phosphorylated Cx43 were also reduced in microvascular (Sato et al., 2002) and retinal (Fernandes et al., 2004) endothelial cells by culture in high glucose for 8–9 days. In diabetic rats, connexin levels are altered in the inferior colliculus (Fig. 4), retina and retinal vasculature (Bobbie et al., 2010), and corpora cavernosa and bladder (Suadicani et al., 2009), whereas the changes in the heart are variable (Howarth et al., 2008; Lin et al., 2006; Makino et al., 2008). Impaired gap junctional communication in endothelial cells, pericytes, and astrocytes suggests that vascular complications of diabetes may affect the central and peripheral nervous systems in addition to the cardiovascular system.

Cx43 in astrocytes may be the major ‘connexin target’ of diabetes—Experimental diabetes reduces dye transfer among astrocytes in tissue culture and in brain slices when assayed with Lucifer yellow VS, Alexa Fluor 350, and 6-NBDG, a non-metabolizable glucose analog (Gandhi et al., 2010; Fig. 6). Gap junctional channels comprised of Cx30 are impermeant to Lucifer yellow CH (Manthey et al., 2001), whereas this dye goes through Cx26 and Cx43 channels (Elfgang et al., 1995). Thus, reduced Lucifer yellow transfer must be related to unidentified changes affecting Cx43 or Cx26 channels, not down-regulation of Cx30 (Figs. 3, 4). Because the inferior colliculus has negligible levels of Cx 26, abnormal Lucifer yellow spreading in these brain slices probably arose from effects of STZ-diabetes on Cx43. The level of Cx43 protein was reduced in the diabetic inferior colliculus, but not in astrocytes grown in high glucose (Figs. 3, 4, 6), implicating other factor(s) in regulation of dye transfer in cultured astrocytes.

S-nitrosylation of Cx43—Astrocytic gap junctional permeability is reduced by induction of nitric oxide synthase and exposure to peroxynitrite (Bolaños and Medina, 1996), findings that are consistent with results of the present study (Fig. 6, Table 2). Reversible S-nitrosylation of Cx43 during severe metabolic inhibition of astrocytes and HeLa cells is associated with increased dye uptake that is ascribed to opening of cell surface hemichannels (Contreras et al., 2002; Retamal et al., 2006, 2007). S-Nitrosylation of Cx43 is also linked to regulation of communication between endothelial cells and vascular smooth muscle cells via the myoendothelial junction in resistance arteries (Straub et al., 2010). The contrasting and apparently-opposing responses of astrocytic cell surface channels and gap junctional channels to reducing agents and nitric oxide donors in the above studies are striking. Severe metabolic blockade opens cell surface channels whereas growth in high glucose does not; dithiothreitol closes the channels opened by prolonged metabolic inhibition, but increases dye coupling in high glucose cultures; and nitric oxide donors inhibit dye transfer among astrocytes grown in low glucose, yet open cell surface channels in the absence of metabolic inhibition. Elucidation of the basis for these differences may provide a better understanding of the complexity of regulation of gap junctional communication among astrocytes in normal brain and under pathophysiological conditions.

Acknowledgments

Grant information: This work was supported by National Institutes of Health grant DK081936 (to GD). The content of the work is solely the responsibility of the authors and does not necessarily represent the official views of the National Institute of Diabetes and Digestive and Kidney Diseases or the National Institutes of Health.

References

Abe T, Takahashi S, Suzuki N. Oxidative metabolism in cultured rat astroglia: effects of reducing the glucose concentration in the culture medium and of D-aspartate or potassium stimulation. J Cereb Blood Flow Metab. 2006; 26:153–160. [PubMed: 15973351]

Aldridge GM, Podrebarac DM, Greenough WT, Weiler IJ. The use of total protein stains as loading controls: an alternative to high-abundance single-protein controls in semi-quantitative immunoblotting. J Neurosci Methods. 2008; 172:250–254. [PubMed: 18571732]

Alegria-Schaffer A, Lodge A, Vattem K. Performing and optimizing Western blots with an emphasis on chemiluminescent detection. Methods Enzymol. 2009; 463:573–99. [PubMed: 19892193]

Allen KV, Frier BM, Strachan MW. The relationship between type 2 diabetes and cognitive dysfunction: longitudinal studies and their methodological limitations. Eur J Pharmacol. 2004; 490:169–175. [PubMed: 15094083]

Atkinson MM, Lampe PD, Lin HH, Kollander R, Li XR, Kiang DT. Cyclic AMP modifies the cellular distribution of connexin43 and induces a persistent increase in the junctional permeability of mouse mammary tumor cells. J Cell Sci. 1995; 108:3079–3090. [PubMed: 8537447]

Ball KK, Gandhi GK, Thrash J, Cruz NF, Dienel GA. Astrocytic connexin distributions and rapid, extensive dye transfer via gap junctions in the inferior colliculus: Implications for [^{14}C]glucose metabolite trafficking. J Neurosci Res. 2007; 85:3267–3283. [PubMed: 17600824]

Bauer DE, Haroutunian V, McCullumsmith RE, Meador-Woodruff JH. Expression of four housekeeping proteins in elderly patients with schizophrenia. J Neural Transm. 2009; 116:487–491. [PubMed: 19139805]

Biessels GJ, Cristino NA, Rutten GJ, Hamers FP, Erkelens DW, Gispen WH. Neurophysiological changes in the central and peripheral nervous system of streptozotocin-diabetic rats. Course of development and effects of insulin treatment. Brain. 1999; 122:757–768. [PubMed: 10219786]

Biessels GJ, Gispen WH. The impact of diabetes on cognition: what can be learned from rodent models? Neurobiol Aging. 2005; 26(Suppl 1):36–41. [PubMed: 16223548]

Biessels GJ, Kamal A, Urban IJ, Spruijt BM, Erkelens DW, Gispen WH. Water maze learning and hippocampal synaptic plasticity in streptozotocin-diabetic rats: effects of insulin treatment. Brain Res. 1998; 800:125–135. [PubMed: 9685609]

Biessels GJ, ter Laak MP, Kamal A, Gispen WH. Effects of the Ca^{2+} antagonist nimodipine on functional deficits in the peripheral and central nervous system of streptozotocin-diabetic rats. Brain Res. 2005; 1035:86–93. [PubMed: 15713280]

Bobbie MW, Roy S, Trudeau K, Munger SJ, Simon AM, Roy S. Reduced connexin 43 expression and its effect on the development of vascular lesions in retinas of diabetic mice. Invest Ophthalmol Vis Sci. 2010; 51:3758–3763. [PubMed: 20130277]

Bolaños JP, Medina JM. Induction of nitric oxide synthase inhibits gap junction permeability in cultured rat astrocytes. J Neurochem. 1996; 66:2091–2099. [PubMed: 8780040]

Brands AM, Biessels GJ, Kappelle LJ, de Haan EH, de Valk HW, Algra A, Kessels RP. Utrecht Diabetic Encephalopathy Study Group. Cognitive functioning and brain MRI in patients with type 1 and type 2 diabetes mellitus: a comparative study. Dement Geriatr Cogn Disord. 2007; 23:343–350. [PubMed: 17374953]

Brissette JL, Kumar NM, Gilula NB, Dotto GP. The tumor promoter 12-O-tetradecanoylphorbol-13-acetate and the ras oncogene modulate expression and phosphorylation of gap junction proteins. Mol Cell Biol. 1991; 11:5364–5371. [PubMed: 1656230]

Brownlee M. The pathobiology of diabetic complications: a unifying mechanism. Diabetes. 2005; 54:1615–1625. [PubMed: 15919781]

Buller N, Laurian N, Shvili I, Laurian L. Delayed brainstem auditory evoked responses in experimental diabetes mellitus. J Laryngol Otol. 1986; 100:883–891. [PubMed: 3746104]

Buller N, Shvili Y, Laurian N, Laurian L, Zohar Y. Delayed brainstem auditory evoked responses in diabetic patients. J Laryngol Otol. 1988; 102:857–860. [PubMed: 2848913]

Burghardt RC, Barhoumi R, Sewall TC, Bowen JA. Cyclic AMP induces rapid increases in gap junction permeability and changes in the cellular distribution of connexin43. J Membr Biol. 1995; 148:243–253. [PubMed: 8747556]

Burt JM, Spray DC. Inotropic agents modulate gap junctional conductance between cardiac myocytes. Am J Physiol. 1988; 254:H1206–1210. [PubMed: 2837915]

Calvo AC, Moreno-Igoa M, Manzano R, Ordovás L, Yagüe G, Oliván S, Muñoz MJ, Zaragoza P, Osta R. Determination of protein and RNA expression levels of common housekeeping genes in a mouse model of neurodegeneration. Proteomics. 2008; 8:4338–4433. [PubMed: 18814324]

Chibber R, Molinatti PA, Kohner EM. Intracellular protein glycation in cultured retinal capillary pericytes and endothelial cells exposed to high-glucose concentration. Cell Mol Biol (Noisy-le-grand). 1999; 45:47–57. [PubMed: 10099839]

Contreras JE, Sánchez HA, Eugenin EA, Speidel D, Theis M, Willecke K, Bukauskas FF, Bennett MV, Sáez JC. Metabolic inhibition induces opening of unapposed connexin 43 gap junction hemichannels and reduces gap junctional communication in cortical astrocytes in culture. Proc Natl Acad Sci USA. 2002; 99:495–500. [PubMed: 11756680]

Cruz NF, Ball KK, Dienel GA. Functional imaging of focal brain activation in conscious rats: impact of [(14)C]glucose metabolite spreading and release. J Neurosci Res. 2007; 85:3254–3266. [PubMed: 17265468]

Jacobson AM, Musen G, Ryan CM, Silvers N, Cleary P, Waberski B, Burwood A, Weinger K, Bayless M, Dahms W, Harth J. Complications Trial/Epidemiology of Diabetes Interventions and Complications Study Research Group. Long-term effect of diabetes and its treatment on cognitive function. N Engl J Med. 2007; 356:1842–1852. [PubMed: 17476010]

Di Mario U, Morano S, Valle E, Pozzessere G. Electrophysiological alterations of the central nervous system in diabetes mellitus. Diabetes Metab Rev. 1995; 11:259–277. [PubMed: 8536543]

Díaz de León-Morales LV, Jáuregui-Renaud K, Garay-Sevilla ME, Hernández-Prado J, Malacara-Hernández JM. Auditory impairment in patients with type 2 diabetes mellitus. Arch Med Res. 2005; 36:507–510. [PubMed: 16099330]

Dienel GA, Cruz NF. Imaging brain activation: simple pictures of complex biology. Ann N Y Acad Sci. 2008; 1147:139–170. [PubMed: 19076439]

Dittmer A, Dittmer J. Beta-actin is not a reliable loading control in Western blot analysis. Electrophoresis. 2006; 27:2844–2845. [PubMed: 16688701]

Du Y, Sarthy VP, Kern TS. Interaction between NO and COX pathways in retinal cells exposed to elevated glucose and retina of diabetic rats. Am J Physiol Regul Integr Comp Physiol. 2004; 287:R735–R741. [PubMed: 15371279]

Elfgang C, Eckert R, Lichtenberg-Frate H, Butterweck A, Traub O, Klein RA, Hülser DF, Willecke K. Specific permeability and selective formation of gap junction channels in connexin-transfected HeLa cells. J Cell Biol. 1995; 129:805–817. [PubMed: 7537274]

Esen N, Tanga FY, DeLeo JA, Kielian T. Toll-like receptor 2 (TLR2) mediates astrocyte activation in response to the Gram-positive bacterium Staphylococcus aureus. J Neurochem. 2004; 88:746–758. [PubMed: 14720224]

Esen N, Shuffield D, Syed MM, Kielian T. Modulation of connexin expression and gap junction communication in astrocytes by the gram-positive bacterium S. aureus. Glia. 2007; 55:104–17. [PubMed: 17029244]

Fernandes R, Girão H, Pereira P. High glucose down-regulates intercellular communication in retinal endothelial cells by enhancing degradation of connexin 43 by a proteasome-dependent mechanism. J Biol Chem. 2004; 279:27219–27224. [PubMed: 15123628]

Freshhney, IR. A manual of basic technique. 4. New York: Wiley-Liss; 2000. Culture of Animal Cells.

Frisina ST, Mapes F, Kim S, Frisina DR, Frisina RD. Characterization of hearing loss in aged type II diabetics. Hear Res. 2006; 211:103–113. [PubMed: 16309862]

Gandhi GK, Ball KK, Cruz NF, Dienel GA. Hyperglycaemia and diabetes impair gap junctional communication among astrocytes. ASN Neuro. 2010; 2(2):art:e00030.10.1042/AN20090048

Ghitescu LD, Gugliucci A, Dumas F. Actin and annexins I and II are among the main endothelial plasmalemma-associated proteins forming early glucose adducts in experimental diabetes. Diabetes. 2001; 50:1666–1674. [PubMed: 11423489]

Greer S, Honeywell R, Geletu M, Arulanandam R, Raptis L. Housekeeping genes; expression levels may change with density of cultured cells. J Immunol Methods. 2010; 355:76–79. [PubMed: 20171969]

Gross PM, Sposito NM, Pettersen SE, Panton DG, Fenstermacher JD. Topography of capillary density, glucose metabolism, and microvascular function within the rat inferior colliculus. J Cereb Blood Flow Metab. 1987; 7:154–160. [PubMed: 3558498]

Hamby ME, Uliasz TF, Hewett SJ, Hewett JA. Characterization of an improved procedure for the removal of microglia from confluent monolayers of primary astrocytes. J Neurosci Methods. 2006; 150:128–137. [PubMed: 16105687]

Hammes HP, Du X, Edelstein D, Taguchi T, Matsumura T, Ju Q, Lin J, Bierhaus A, Nawroth P, Hannak D, Neumaier M, Bergfeld R, Giardino I, Brownlee M. Benfotiamine blocks three major pathways of hyperglycemic damage and prevents experimental diabetic retinopathy. Nat Med. 2003; 9:294–299. [PubMed: 12592403]

Hara MR, Snyder SH. Nitric oxide-GAPDH-Siah: a novel cell death cascade. Cell Mol Neurobiol. 2006; 26:527–538. [PubMed: 16633896]

Hara MR, Cascio MB, Sawa A. GAPDH as a sensor of NO stress. Biochim Biophys Acta. 2006; 1762:502–509. [PubMed: 16574384]

Hertz L, Peng L, Lai JC. Functional studies in cultured astrocytes. Methods. 1998; 16:293–310. [PubMed: 10071068]

Hossain MZ, Murphy LJ, Hertzberg EL, Nagy JI. Phosphorylated forms of connexin43 predominate in rat brain: demonstration by rapid inactivation of brain metabolism. J Neurochem. 1994; 62:2394–2403. [PubMed: 8189244]

Howarth FC, Chandler NJ, Kharche S, Tellez JO, Greener ID, Yamanushi TT, Billeter R, Boyett MR, Zhang H, Dobrzynski H. Effects of streptozotocin-induced diabetes on connexin43 mRNA and protein expression in ventricular muscle. Mol Cell Biochem. 2008; 319:105–114. [PubMed: 18629610]

Huber JD, VanGilder RL, Houser KA. Streptozotocin-induced diabetes progressively increases blood-brain barrier permeability in specific brain regions in rats. Am J Physiol Heart Circ Physiol. 2006; 291:H2660–H2668. [PubMed: 16951046]

Inoguchi T, Ueda F, Umeda F, Yamashita T, Nawata H. Inhibition of intercellular communication via gap junction in cultured aortic endothelial cells by elevated glucose and phorbol ester. Biochem Biophys Res Commun. 1995; 208:492–497. [PubMed: 7695598]

Kamal A, Biessels GJ, Urban IJ, Gispen WH. Hippocampal synaptic plasticity in streptozotocin-diabetic rats: impairment of long-term potentiation and facilitation of long-term depression. Neurosci. 1999; 90:737–745.

Kamal A, Biessels GJ, Gispen WH, Ramakers GM. Synaptic transmission changes in the pyramidal cells of the hippocampus in streptozotocin-induced diabetes mellitus in rats. Brain Res. 2006; 1073–1074:276–280.

Kanwar M, Kowluru RA. Role of glyceraldehyde 3-phosphate dehydrogenase in the development and progression of diabetic retinopathy. Diabetes. 2009; 58:227–234. [PubMed: 18852331]

Kleman AM, Yuan JY, Aja S, Ronnett GV, Landree LE. Physiological glucose is critical for optimized neuronal viability and AMPK responsiveness in vitro. J Neurosci Methods. 2008; 167:292–301. [PubMed: 17936912]

Kodl CT, Seaquist ER. Cognitive dysfunction and diabetes mellitus. Endocr Rev. 2008; 29:494–511. [PubMed: 18436709]

Kornberg MD, Sen N, Hara MR, Juluri KR, Nguyen JV, Snowman AM, Law L, Hester LD, Snyder SH. GAPDH mediates nitrosylation of nuclear proteins. Nat Cell Biol. 2010; 12:1094–1100. [PubMed: 20972425]

Kuroki T, Inoguchi T, Umeda F, Ueda F, Nawata H. High glucose induces alteration of gap junction permeability and phosphorylation of connexin-43 in cultured aortic smooth muscle cells. Diabetes. 1998; 47:931–936. [PubMed: 9604871]

Kusner LL, Sarthy VP, Mohr S. Nuclear translocation of glyceraldehyde-3-phosphate dehydrogenase: a role in high glucose-induced apoptosis in retinal Müller cells. Invest Ophthalmol Vis Sci. 2004; 45:1553–1561. [PubMed: 15111614]

Lampe PD, Lau AF. The effects of connexin phosphorylation on gap junctional communication. Int J Biochem Cell Biol. 2004; 36:1171–1186. [PubMed: 15109565]

Leal EC, Manivannan A, Hosoya K, Terasaki T, Cunha-Vaz J, Ambrósio AF, Forrester JV. Inducible nitric oxide synthase isoform is a key mediator of leukostasis and blood-retinal barrier breakdown in diabetic retinopathy. Invest Ophthalmol Vis Sci. 2007; 48:5257–5265. [PubMed: 17962481]

Li AF, Sato T, Haimovici R, Okamoto T. High glucose alters connexin 43 expression and gap junction intercellular communication activity in retinal pericytes. Invest Ophthalmol Vis Sci. 2003; 44:5376–5382. [PubMed: 14638741]

Li W, Hertzberg EL, Spray DC. Regulation of connexin43-protein binding in astrocytes in response to chemical ischemia/hypoxia. J Biol Chem. 2005; 280:7941–7948. [PubMed: 15618229]

Li WE, Nagy JI. Connexin43 phosphorylation state and intercellular communication in cultured astrocytes following hypoxia and protein phosphatase inhibition. Eur J Neurosci. 2000; 12:2644–2650. [PubMed: 10947839]

Lin H, Ogawa K, Imanaga I, Tribulova N. Remodeling of connexin 43 in the diabetic rat heart. Mol Cell Biochem. 2006; 290:69–78. [PubMed: 16633735]

Little AA, Edwards JL, Feldman EL. Diabetic neuropathies. Pract Neurol. 2007; 7:82–92. [PubMed: 17430872]

Liu NK, Xu XM. Beta-tubulin is a more suitable internal control than beta-actin in western blot analysis of spinal cord tissues after traumatic injury. J Neurotrauma. 2006; 23:1794–1801. [PubMed: 17184189]

Makino A, Platoshyn O, Suarez J, Yuan JX, Dillmann WH. Downregulation of connexin40 is associated with coronary endothelial cell dysfunction in streptozotocin-induced diabetic mice. Am J Physiol Cell Physiol. 2008; 295:C221–C230. [PubMed: 18463230]

Malfait M, Gomez P, van Veen TA, Parys JB, De Smedt H, Vereecke J, Himpens B. Effects of hyperglycemia and protein kinase C on connexin43 expression in cultured rat retinal pigment epithelial cells. J Membr Biol. 2001; 181:31–40. [PubMed: 11331935]

Manschot SM, Gispen WH, Kappelle LJ, Biessels GJ. Nerve conduction velocity and evoked potential latencies in streptozotocin-diabetic rats: effects of treatment with an angiotensin converting enzyme inhibitor. Diabetes Metab Res Rev. 2003; 19:469–477. [PubMed: 14648806]

Manschot SM, Biessels GJ, Rutten GE, Kessels RC, Gispen WH, Kappelle LJ. Utrecht Diabetic Encephalopathy Study Group. Peripheral and central neurologic complications in type 2 diabetes mellitus: no association in individual patients. J Neurol Sci. 2008; 264:157–162. [PubMed: 17850822]

Manthey D, Banach K, Desplantez T, Lee CG, Kozak CA, Traub O, Weingart R, Willecke K. Intracellular domains of mouse connexin26 and -30 affect diffusional and electrical properties of gap junction channels. J Membr Biol. 2001; 181:137–148. [PubMed: 11420600]

McCall AL. The impact of diabetes on the CNS. Diabetes. 1992; 41:557–570. [PubMed: 1568525]

McCall AL. Cerebral glucose metabolism in diabetes mellitus. Eur J Pharmacol. 2004; 490:147–158. [PubMed: 15094081]

McCall AL. Altered glycemia and brain-update and potential relevance to the aging brain. Neurobiol Aging. 2005; 26(Suppl 1):70–75. [PubMed: 16198444]

Mîinea C, Kuruvilla R, Merrikh H, Eichberg J. Altered arachidonic acid biosynthesis and antioxidant protection mechanisms in Schwann cells grown in elevated glucose. J Neurochem. 2002; 81:1253–1262. [PubMed: 12068073]

Mooradian AD. Pathophysiology of central nervous system complications in diabetes mellitus. Clin Neurosci. 1997; 4:322–326. [PubMed: 9358975]

Nagy JI, Li X, Rempel J, Stelmack G, Patel D, Staines WA, Yasumura T, Rash JE. Connexin26 in adult rodent central nervous system: demonstration at astrocytic gap junctions and colocalization with connexin30 and connexin43. J Comp Neurol. 2001; 441:302–323. [PubMed: 11745652]

Nagy JI, Rash JE. Connexins and gap junctions of astrocytes and oligodendrocytes in the CNS. Brain Res Brain Res Rev. 2000; 32:29–44. [PubMed: 10751655]

Oku H, Kodama T, Sakagami K, Puro DG. Diabetes-induced disruption of gap junction pathways within the retinal microvasculature. Invest Ophthalmol Vis Sci. 2001; 42:1915–1920. [PubMed: 11431461]

Paulson AF, Lampe PD, Meyer RA, TenBroek E, Atkinson MM, Walseth TF, Johnson RG. Cyclic AMP and LDL trigger a rapid enhancement in gap junction assembly through a stimulation of connexin trafficking. J Cell Sci. 2000; 113:3037–3049. [PubMed: 10934042]

Prime G, Horn G, Sutor B. Time-related changes in connexin mRNA abundance in the rat neocortex during postnatal development. Brain Res Dev Brain Res. 2000; 119:111–125.

Rash JE, Yasumura T, Dudek FE, Nagy JI. Cell-specific expression of connexins and evidence of restricted gap junctional coupling between glial cells and between neurons. J Neurosci. 2001; 21:1983–2000. [PubMed: 11245683]

Retamal MA, Cortés CJ, Reuss L, Bennett MV, Sáez JC. S-nitrosylation and permeation through connexin 43 hemichannels in astrocytes: induction by oxidant stress and reversal by reducing agents. Proc Natl Acad Sci USA. 2006; 103:4475–4480. [PubMed: 16537412]

Retamal MA, Schalper KA, Shoji KF, Bennett MV, Sáez JC. Opening of connexin 43 hemichannels is increased by lowering intracellular redox potential. Proc Natl Acad Sci USA. 2007; 104:8322–8327. [PubMed: 17494739]

Roberts RO, Geda YE, Knopman DS, Christianson TJ, Pankratz VS, Boeve BF, Vella A, Rocca WA, Petersen RC. Association of duration and severity of diabetes mellitus with mild cognitive impairment. Arch Neurol. 2008; 65:1066–1073. [PubMed: 18695056]

Romero-Calvo I, Ocón B, Martínez-Moya P, Suárez MD, Zarzuelo A, Martínez-Augustin O, de Medina FS. Reversible Ponceau staining as a loading control alternative to actin in Western blots. Anal Biochem. 2010; 401:318–320. [PubMed: 20206115]

Rubini R, Biasiolo F, Fogarolo F, Magnavita V, Martini A, Fiori MG. Brainstem auditory evoked potentials in rats with streptozotocin-induced diabetes. Diabetes Res Clin Pract. 1992; 16:19–25. [PubMed: 1576928]

Saez JC, Spray DC, Nairn AC, Hertzberg E, Greengard P, Bennett MV. cAMP increases junctional conductance and stimulates phosphorylation of the 27-kDa principal gap junction polypeptide. Proc Natl Acad Sci USA. 1986; 83:2473–2477. [PubMed: 3010311]

Sato T, Haimovici R, Kao R, Li AF, Roy S. Downregulation of connexin 43 expression by high glucose reduces gap junction activity in microvascular endothelial cells. Diabetes. 2002; 51:1565–1571. [PubMed: 11978657]

Schousboe, A.; Nissen, C.; Bock, E.; Sapirstein, VS.; Juurlink, BHJ.; Hertz, L. Biochemical development of rodent astrocytes in primary cultures. In: Giacobini, E.; Vermadalos, A.; Shahar, A., editors. Tissue Culture in Neurobiology. New York: Raven Press; 1980. p. 397-410.

Sen N, Hara MR, Ahmad AS, Cascio MB, Kamiya A, Ehmsen JT, Agrawal N, Hester L, Doré S, Snyder SH, Sawa A. GOSPEL: a neuroprotective protein that binds to GAPDH upon S-nitrosylation. Neuron. 2009; 63:81–91. [PubMed: 19607794]

Sima AA, Kamiya H, Li ZG. Insulin, C-peptide, hyperglycemia, and central nervous system complications in diabetes. Eur J Pharmacol. 2004; 490:187–197. [PubMed: 15094085]

Simmons ML, Murphy S. Induction of nitric oxide synthase in glial cells. J Neurochem. 1992; 59:897–905. [PubMed: 1379633]

Sokoloff L, Reivich M, Kennedy C, Des Rosiers MH, Patlak CS, Pettigrew KD, Sakurada O, Shinohara M. The [^{14}C]deoxyglucose method for the measurement of local cerebral glucose utilization: theory, procedure, and normal values in the conscious and anesthetized albino rat. J Neurochem. 1977; 28:897–916. [PubMed: 864466]

Spray DC, Moreno AP, Kessler JA, Dermietzel R. Characterization of gap junctions between cultured leptomeningeal cells. Brain Res. 1991; 568:1–14. [PubMed: 1667612]

Stalmans P, Himpens B. Effect of increasing glucose concentrations and protein phosphorylation on intercellular communication in cultured rat retinal pigment epithelial cells. Invest Ophthalmol Vis Sci. 1997; 38:1598–1609. [PubMed: 9224288]

Straub AC, Billaud M, Johnstone SR, Best AK, Yemen S, Dwyer ST, Looft-Wilson R, Lysiak JJ, Gaston B, Palmer L, Isakson BE. Compartmentalized connexin 43 S-nitrosylation/denitrosylation regulates heterocellular communication in the vessel wall. Arterioscler Thromb Vasc Biol. 2010 Nov 11. [Epub ahead of print]. 10.1161/ATVBAHA.110.215939

Suadicani SO, Urban-Maldonado M, Tar MT, Melman A, Spray DC. Effects of ageing and streptozotocin-induced diabetes on connexin43 and P2 purinoceptor expression in the rat corpora cavernosa and urinary bladder. BJU Int. 2009; 103:1686–1693. [PubMed: 19154470]

Tay HL, Ray N, Ohri R, Frootko NJ. Diabetes mellitus and hearing loss. Clin Otolaryngol Allied Sci. 1995; 20:130–134. [PubMed: 7634518]

TenBroek EM, Lampe PD, Solan JL, Reynhout JK, Johnson RG. Ser364 of connexin43 and the upregulation of gap junction assembly by cAMP. J Cell Biol. 2001; 155:1307–1318. [PubMed: 11756479]

Thi MM, Urban-Maldonado M, Spray DC, Suadicani SO. Intercellular communication among astrocytes is enhanced by high glucose exposure in culture. 2010 Transactions of the American Society for Neurochemistry. 2010:106.

Tristan C, Shahani N, Sedlak TW, Sawa A. The diverse functions of GAPDH: Views from different subcellular compartments. Cell Signal. 2010 Aug 19. [Epub ahead of print].

Vaughan N, James K, McDermott D, Griest S, Fausti S. A 5-year prospective study of diabetes and hearing loss in a veteran population. Otol Neurotol. 2006; 27:37–43. [PubMed: 16371845]

Vaughan N, James K, McDermott D, Griest S, Fausti S. Auditory brainstem response differences in diabetic and non-diabetic veterans. J Am Acad Audiol. 2007; 18:863–871. [PubMed: 18496995]

Weldon S, Ambroz K, Schutz-Geschwender A, Olive DM. Near-infrared fluorescence detection permits accurate imaging of loading controls for Western blot analysis. Anal Biochem. 2008; 375:156–158. [PubMed: 18162169]

Yego EC, Mohr S. siah-1 Protein is necessary for high glucose-induced glyceraldehyde-3-phosphate dehydrogenase nuclear accumulation and cell death in Muller cells. J Biol Chem. 2010; 285:3181–3190. [PubMed: 19940145]

Yego EC, Vincent JA, Sarthy V, Busik JV, Mohr S. Differential regulation of high glucose-induced glyceraldehyde-3-phosphate dehydrogenase nuclear accumulation in Müller cells by IL-1beta and IL-6. Invest Ophthalmol Vis Sci. 2009; 50:1920–1928. [PubMed: 19060282]

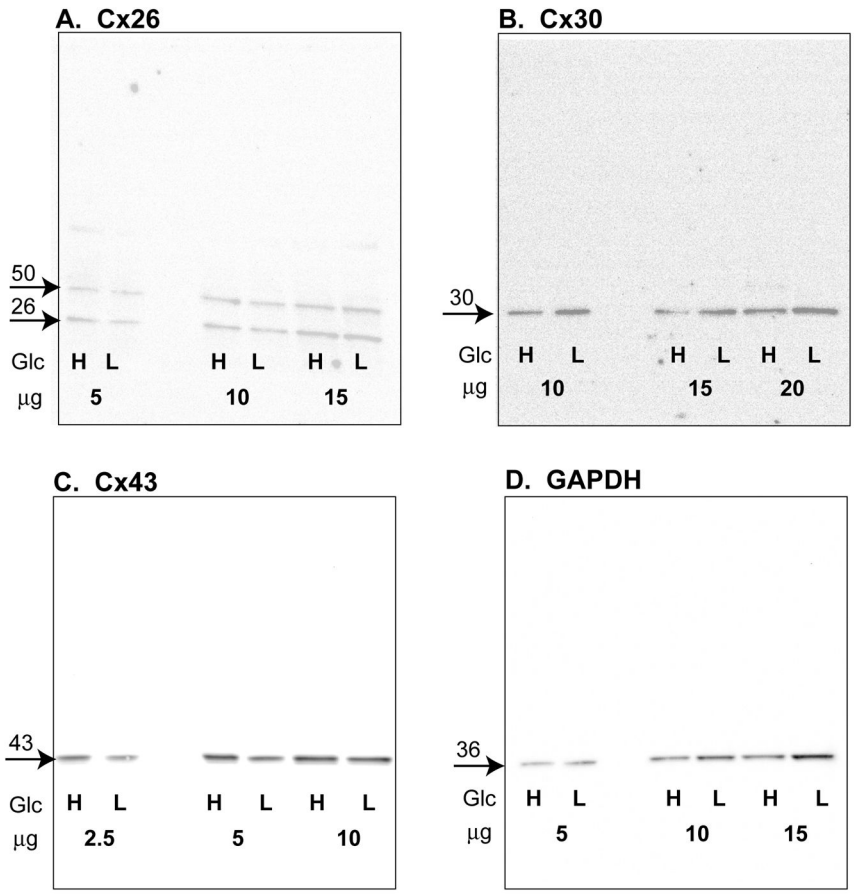

Fig. 1. Western blots from paired extracts of astrocytes grown in high or low glucose

Extracts were prepared from each batch of cultured astrocytes in which cells were grown in low (L) (5.5 mmol/L) or high (H) (25 mmol/L) glucose (Glc). For each sample pair of each batch, the assay for each protein of interest was carried out by loading the same amount of extract protein for the high-low glucose pair into adjacent lanes of the gel. Three protein amounts over the range 2.5–20 µg were loaded on each gel, as indicated below each sample pair. The blots were first probed with an antibody against (A) connexin 26 (Cx26), (B) connexin 30 (Cx30), or (C) connexin 43 (Cx43), then stripped and probed for (D) glyceraldehyde-3-phosphate dehydrogenase (GAPDH). Each gel also contained molecular weight standards (not shown), and approximate molecular weights (kDa) of proteins of interest are indicated above the arrows in left margin of each panel; these values were determined in each gel by graphical analysis of semi-log plots of molecular weights of the protein standards and migration distances (relative to the dye front) of the standards and of proteins of interest. The boxed areas contain the entire blot and demonstrate that, except for Cx26, one predominant band was visualized for each connexin. Most, but not all, Cx26 gels showed two bands that, when present, had similar intensity levels; the band with the higher molecular weight (~50 kDa) may represent a dimer.

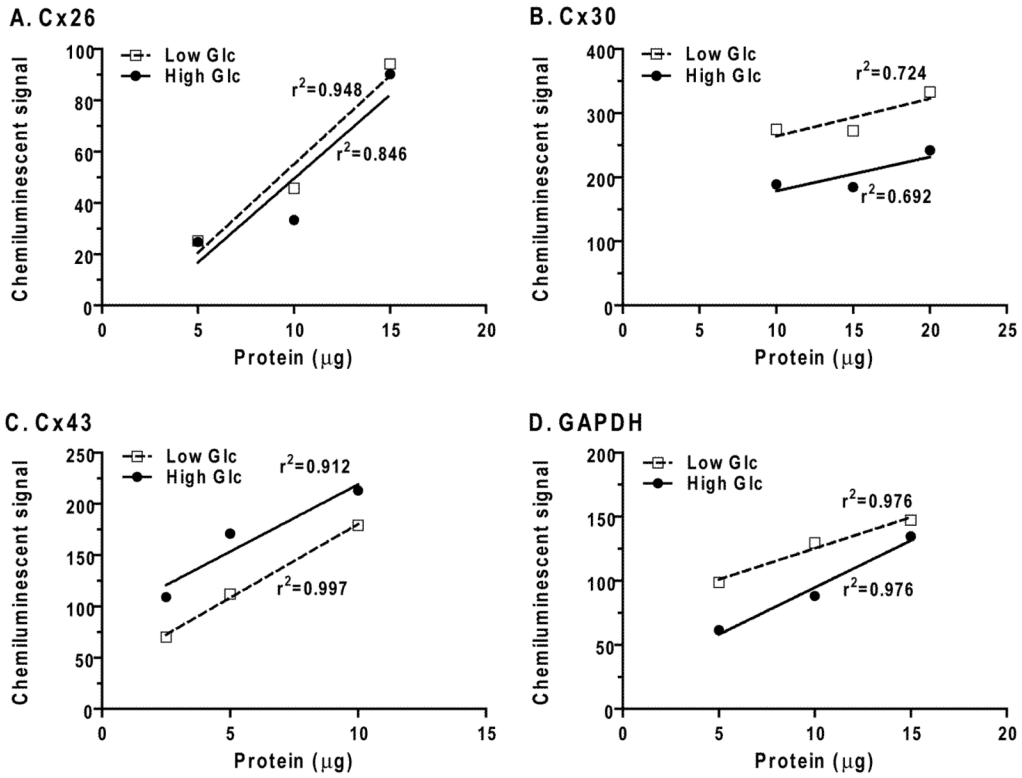

Fig. 2. Relationships of chemiluminescent signals to protein amount loaded on the gel

Three amounts of protein from extracts of pairs of high and low glucose cultures were loaded onto adjacent lanes in each gel (see Fig. 1), separated by electrophoresis, transferred to membranes, and chemiluminescent signals captured (BioRad ChemiDoc system) and analyzed (MCID Elite™ software). Background-subtracted signals (arbitrary units) are plotted against the loaded protein amount for extracts from high and low glucose cultures.

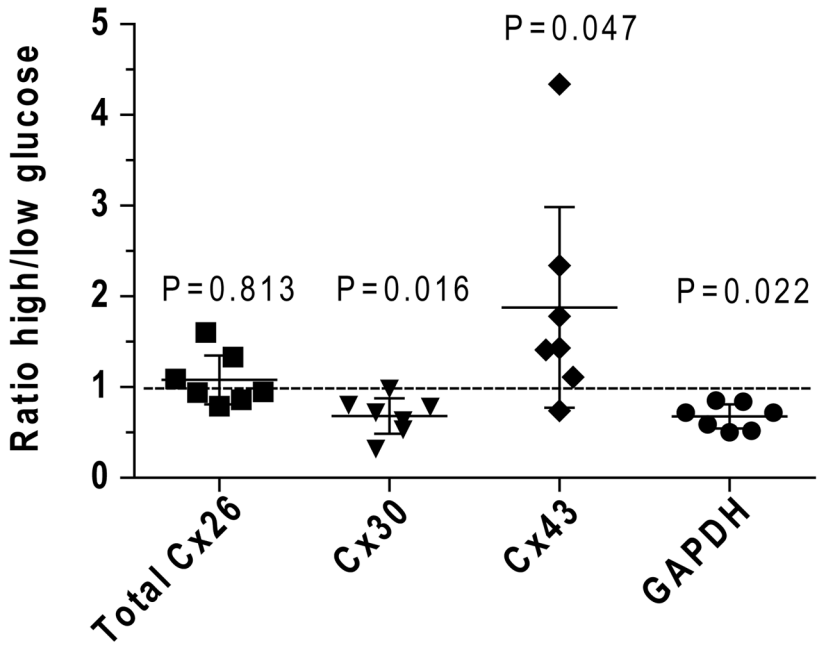

Fig. 3. Growth of cultured astrocytes in high glucose medium differentially affects connexin (Cx) and glyceraldehyde-3-phosphate dehydrogenase (GAPDH) protein levels

Western blots of each sample (n=7 independent batches of astrocytes grown in high and low glucose) were assayed in triplicate for each Cx protein by application of different extract protein amounts per gel (2.5, 5, 10, 15, and/or 20 μg/lane, see Figs. 1 and 2). Immunoreactive GAPDH was assayed after stripping each Cx blot and re-probing with antibodies against GAPDH. After background subtraction, the ratio of the signal intensity for each band in the sample derived from astrocytes grown in high glucose to that in cells grown in low glucose was calculated for each protein concentration loaded onto the gel, and the values were averaged for that sample. The mean ratio for each sample pair was used to calculate the overall mean and variance for the seven culture batches grown in high or low glucose for each protein of interest. For Cx26, the signals for the two bands in each sample were combined and used to calculate the ratio for that sample pair. Values for each sample are shown; horizontal lines are mean ratios and vertical bars are ±95% confidence intervals. Statistically significant differences from a ratio of 1.0 (dashed line) were identified by the Wilcoxon signed rank test (one sample t test); P values are indicated.

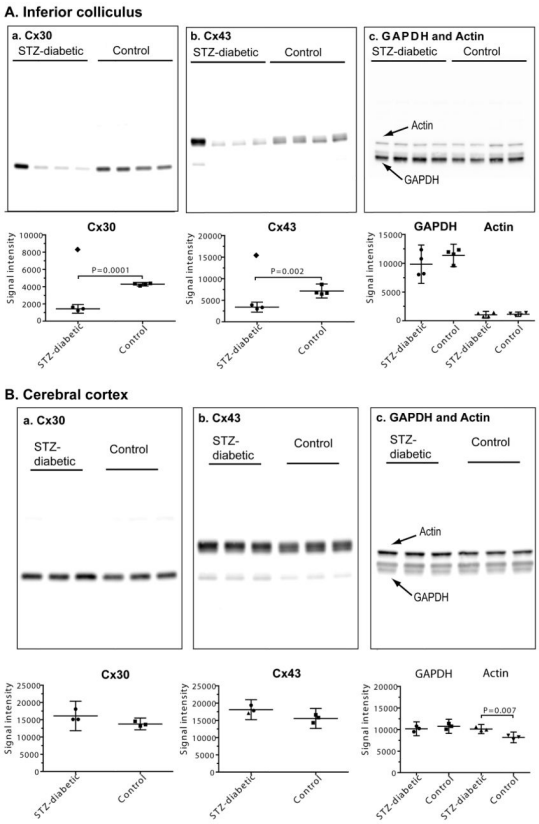

Fig. 4. Western blots showing regional selectivity of changes in levels of Cx30 and Cx43 in brain of streptozotocin (STZ)-diabetic rats at 5–6 months after onset of diabetes

Samples of (**A**) inferior colliculus (n = 4/group) and (**B**) cerebral cortex (n = 3/group) from age-matched, vehicle-injected control and STZ-diabetic rats were assayed for Cx30 (**a**), Cx43 (**b**) and GAPDH and actin (**c**). The same amount of total protein from different tissue extract samples was loaded onto SDS-PAGE gels (upper panels in A and B) and Western blots were probed with antibodies against the indicated proteins. Separate gels and blots were used for assays of actin (43 kDa) and GAPDH (36 kDa), and each blot was probed with both antibodies.

Chemiluminescent signal intensities are in the lower panels of A and B. Values for each sample are shown; horizontal lines are mean ratios and vertical bars are ±95% confidence intervals. All samples were assayed on at least two replicate gels with all samples for each protein of interest on the same gel. (**A**) Note that one diabetic rat had a very high signal intensity in the Cx30 and Cx43 blots of samples of inferior colliculus (lane 1 from the left in the upper panels, denoted by filled diamonds in the lower panels) that was about twice that of the respective control mean (lower panels) and was even higher than the respective mean values for Cx30 and Cx43 in the other three rats; these two values were identified as a significant outliers (Grubbs test) from the other three values, and were not used to calculate mean values for diabetic Cx30 and Cx43 intensities. Statistically significant differences were identified by the t test; P values are indicated. In sharp contrast, the signal intensities for GAPDH and actin in the same outlier rat were similar to the other diabetic and control values (panel A–c, upper and lower panels), indicating that the connexin proteins, not other proteins in the same extract diverged from the rest of the samples in the group. Signal intensities for the three rats with low levels of immunoreactive Cx30 and Cx43 protein were also normalized relative to actin or GAPDH in the same sample (data not shown). When these normalized diabetic and control samples were compared (t test), the p values were as

follows: Cx43/actin (p=0.034), Cx43/GAPDH (p=0.051), Cx30/actin (p=0.009), Cx30/GAPDH (p=0.005). Thus, Cx30 and Cx43 levels were significantly reduced, whether expressed relative to the amount of extract protein loaded onto the gel or to other proteins in the same samples. The rat with high levels of immunoreactive Cx30 and Cx43 protein also had higher-than-normal ratios when expressed relative to actin and GAPDH (see Table 1c). (**B**) Note that two immunoreactive bands were visible for GAPDH, and the bar graphs include both bands; a minor, lower molecular weight band for Cx43 was visible in the blots but was not assayed. When signal intensities for Cx30 and Cx43 were expressed relative to those for GAPDH or actin, there were no statistically significant differences between diabetic and control rats even though the level of immunoreactive actin was about 24% higher in the diabetic tissue (t test; P value indicated), normalized to loaded protein amount.

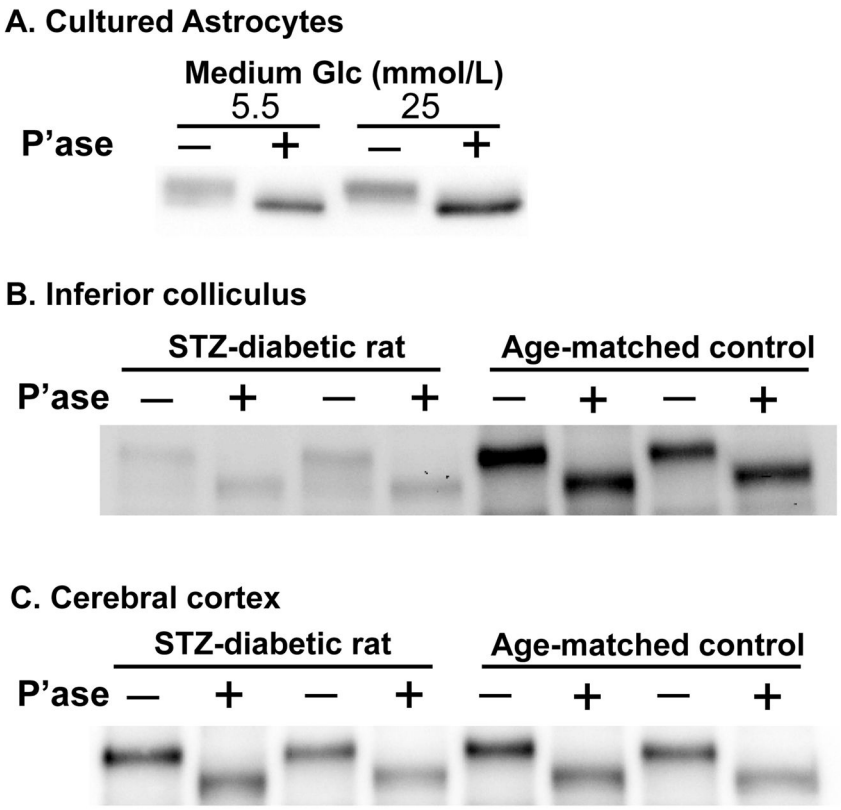

Fig. 5. Representative Western blots showing that most of the Cx43 is phosphorylated in astrocytes in control conditions and experimental diabetes

Extracts from astrocytes cultured in high (25 mmol/L) or low (5.5 mmol/L) glucose (Glc) for 2 weeks (A) and from inferior colliculus (B) and cerebral cortex (C) from STZ-diabetic rats and vehicle-treated, age-matched controls were incubated with buffer or alkaline phosphatase (P'ase), then assayed in duplicate. Buffer and P'ase are denoted as − and + respectively.

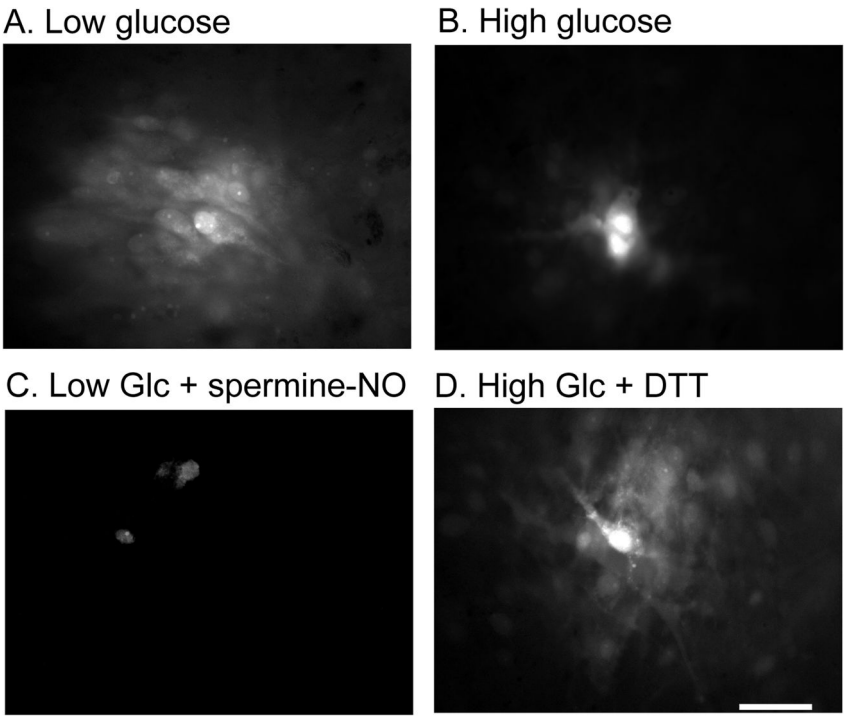

Fig. 6. Lucifer yellow labeling in astrocyte cultures grown in low and high glucose

Astrocytes were grown in culture medium containing low (5.5 mmol/L, A, C) or high (25 mmol/L, B, D) glucose for two weeks. Single astrocytes were impaled with a micropipette containing 4% Lucifer yellow, and the dye was allowed to diffuse for 2 min, and dye-labeled area measured (see Table 2). (C) Astrocytes grown in low glucose were treated with spermine-NO (250 μmol/L for 1h) prior to dye transfer assay. (D) Astrocytes grown in high glucose were treated with dithiothreitol (DTT, 10 mmol/L for 10 min) prior to dye transfer assay. The scale bar represents 40 μm and applies to all panels.

Table 1

Effect of boiling and reproducibility of chemiluminescent signals in replicate assays.

Test condition	Cx43	Cx30	Cx26	GAPDH	Actin
a. Boiled/non-boiled ratio[a]					
High glucose cultures	0.43, 0.26	1.41,1.02, 1.27		0.67, 0.66, 0.56	
Low glucose cultures	0.35, 0.13	1.13, 0.94, 0.88	0.81, 0.74, 0.32	0.60, 0.43, 0.36	0.30, 0.34
b. Duplicates on same gel[b]	1.09 ± 0.09 (12, 8%)			1.01, 1.01	1.34, 1.34
c. Replicates on different gels[c]					
Pair 1	2.24 ± 0.14 (4, 6%)	1.50, 1.85		1.10 ± 0.15 (5, 14%)	1.43 ± 0.27 (5, 19%)
Pair 2	0.44 ± 0.05 (3, 10%)	0.33, 0.37		0.99 ± 0.24 (4, 24%)	1.17 ± 0.14 (4, 12%)
Pair 3	0.44 ± 0.03 (4, 6%)	0.34, 0.35		0.72 ± 0.28 (5, 39%)	0.53 ± 0.14 (5, 26%)
Pair 4	0.43 ± 0.04 (4, 9%)	0.29, 0.28		0.87 ± 0.15 (5, 18%)	0.59 ± 0.25 (5, 43%)

[a] Two aliquots of an extract from cultured astrocytes were mixed with sample buffer (see Methods), and one sample was boiled prior to loading the same amount of protein from each sample onto different lanes of the same gel. Values are ratios of chemiluminescent signal in the boiled sample to that for the non-boiled sample; each ratio represents a different extract.

[b] The same amount of non-boiled protein was loaded onto two lanes of the same gel, and the relative chemiluminescent signal for each duplicate pair is expressed as a ratio, calculated by dividing the higher value by the lower one. For Cx43, samples from 12 extracts from cultured astrocytes were assayed on different gels; ratios are mean ± SD (n, cv); the coefficient of variation (cv, expressed as percent) = 100*SD/mean. Each ratio for GAPDH (glyceraldehyde-3-phosphate dehydrogenase) and actin represents a separate sample.

[c] Pairs of samples from the inferior colliculus were assayed on the same gel/blot, and the chemiluminescent signal for diabetic sample was normalized to its corresponding control. Ratios for the same diabetic and control sample pair were determined in 3–5 replicate blots from either (i) pair-wise assays of one diabetic and one control sample on each gel as described in Figs 1 and 2, or (ii) assays for each protein of interest with all diabetic and control samples on the same gel as described in Fig. 4. Ratios are either the mean ± SD (n, cv) for the number of samples for diabetic-control sample pairs or values for separate samples. Note that, on average, the cv for replicate diabetic/control ratios was higher for actin and GAPDH than for Cx43 and for the duplicate assays of Cx30. Note that pair 1 represents the diabetic outlier sample from the one rat that had high levels of Cx43 and Cx30 compared to the other three diabetic rats that had Cx43 and Cx30 levels lower than those of the controls (see Fig. 4).

Table 2

Effect of dithiothreitol and nitric oxide donors on Lucifer yellow-labeled area.

Culture batch	Culture condition	Lucifer yellow-labeled area (μm^2)	Percent
1	Low Glucose	20,110 ± 8,302 (n=11)	100
	High Glucose	5,303 ± 4,810 (n=17)*	26
	High Glucose + dithiothreitol	21,103 ± 7,776 (n=21)	105
2	Low Glucose	12,907 ± 6,718 (n=22)	100
	Low Glucose + nitroprusside	4,573 ± 3,557 (n=27)**	35
3	Low Glucose	5,581 ± 3,463 (n=44)	100
	Low Glucose + spermine-NO	2,947 ± 1,380 (n=28)**	53

Separate batches of astrocytes were grown for 2 weeks in low (5.5 mmol/L) or high (25 mmol/L) glucose. Lucifer yellow-labeled area was assayed on day 14 by impaling a single cell with a micropipette containing 4% Lucifer yellow VS (62 mmol/L) and allowing the dye to diffuse for 2 min (see Fig. 6). Immediately prior to the dye transfer assay, high glucose cultures were treated with vehicle or dithiothreitol (DTT; 10 mmol/L) for 10 min. Separate batches of low glucose cultures were treated with vehicle and either sodium nitroprusside (200 μmol/L) or spermine-NO (250 μmol/L). The vehicle and nitric oxide donors were added to the culture medium and cells were returned to the CO_2 incubator for 1h prior to the dye-transfer assay. Values are means ± SD for the number of samples indicated.

*, p<0.001 vs. DTT or 5.5 mM glucose, ANOVA and Bonferroni test;

**, p<0.001 vs. respective control group, t test.